

Optically Anisotropic Films of Colloidal Nanocrystals/Photoluminescent Dye Doped Polymers

Zeynep Dikmen* 

Eskisehir Osmangazi University, Faculty of Engineering, Department of Biomedical Engineering, Eskisehir 26040, Türkiye

*zeynilmaz@ogu.edu.tr

* Orcid No: 0000-0002-1365-6573

Received: 22 November 2023

Accepted: 9 March 2024

DOI: 10.18466/cbayarfbe.1394435

Abstract

Semiconductor colloidal nanocrystals are attractive materials since they can be adapted to polymers to form hybrid materials and are compatible with many optical applications. Here, synthesis of CdSe/CdS nanorods (NRs) via hot injection method is carried out, followed by preparation of hybrid polymer films from polyethylene glycol monomethyl ether-*block*-poly(glycidyl methacrylate)-*block*-poly[2-(diethylamino)ethyl methacrylate] triblock copolymer (MPEG-*b*-PGMA-*b*-DEAEMA) at a liquid-air interface. The optical properties of the films are finely adjusted to form optically anisotropic (i.e. dual-color emissive) films by using dyes for the other emitter as desired. Thiazolo[5,4-*d*] thiazole (TTz)-based dye and 6-carboxy fluorescein were used for this purpose. Tunable emission of TTz dye from blue to green dependent on changing pH value resulted in blue-green emissive polymer films, while red emission of CdSe/CdS NRs caused red emissive films. Phase separation of these materials is achieved by the hexane-insoluble nature of MPEG-*b*-PGMA-*b*-DEAEMA and the high solubility of NRs in it. These dual emissive films are promising candidates for waveguides and optical sensors.

Keywords: Optically anisotropic film, CdSe/CdS nanorods, dual emissive films, confocal microscopy

1. Introduction

Colloidal nanocrystals can be described as a hybrid material consisting of an inorganic core coated with a layer of organic molecules (ligands). Semiconductor nanocrystals are unique materials with extended optical properties such as high quantum yield, narrow full-width half maximum, and tunable emission wavelength. Such materials are great as dopants for various matrixes to get functional materials. Polymers are quite advantageous as matrix materials for nanocrystals due to their low cost, simple processability, and availability on an industrial scale. Dielectric polymers such as polydimethylsiloxane, polystyrene, and polyacrylates can be used as a matrix for semiconductor nanocrystals due to their optical transparency in the visible region, mechanical strength, flexibility, and their well-known chemical behavior. There are various strategies for incorporating colloidal nanocrystals into polymer matrixes without substantially altering their initial photophysical properties. One of the most widely used and simplest ways is to mix hydrophobic nanocrystals directly as-synthesized with a polymer solution in nonpolar solvents and then evaporate

the solvent to form the mixture to form a solid matrix. Another approach is to disperse nanoparticles in monomers or pre-polymerized oligomers and perform in-situ polymerization to obtain nanocomposites with embedded nanocrystals¹. The most used polymer matrix materials, such as polyacrylates and polystyrene derivatives, limit the potential applications of nanocrystals because of their solid matrixes. Polymethylmethacrylate (PMMA) is used as a matrix for CdSe colloidal quantum wells,² a homogenous CuZnInS (CZIS) nanocrystal-embedded polystyrene with high quantum yield is reported in the earlier studies^{1,3}. In addition to these solid matrixes, CdSe/CdS nanorods were embedded into the flexible polymer to form a film to orient the nanorods by stretching the film, resulting in a higher emission intensity⁴. CdS quantum dot doped polymers were investigated effectively for further applications⁵. Polymer / nanocrystal-based hybrid structures with unique optical properties were also obtained by encapsulating nanocrystals with amphiphilic polymers^{6,7}. Photoluminescent polymers have been prepared by various approaches in the early reports. In the 1980s, Dy³⁺, Er³⁺, Eu³⁺, Tb³⁺, and Sm³⁺ doped

copolymers were prepared to prepare fluorescence polymer materials, and their optical properties, which vary with the thickness and dopant amount of the films were examined⁸⁻¹⁰. Combining copolymers with fluorescent structures such as N-vinyl carbazole-containing vinyl groups has been another strategy to prepare fluorescent polymers in these years^{11,12}. In other reports, fluorescence polymers were prepared by adding dyes to polymers to investigate the effect of the polymer matrix on the Stokes shifts of the fluorophore^{13,14}. By enabling the radical formation of polymers with an initiator such as 9-fluorenyl lithium or by reacting a polymer with a polymeric active end group such as poly(styryl)lithium with a fluorescence monomer such as 1-phenyl-1-(1-pyrenyl)ethylene, the fluorescence molecule is attached to the polymers as an end group^{15,16}. Organic small photoluminescent dyes are well-known materials to prepare highly emissive polymer materials¹⁷. Thiazolo[5,4-*d*]thiazole (TTz)-based fluorophores are one of the most attractive fluorophores since they have exhibited solvatochromic effect¹⁸, excited-state intramolecular proton transfer (ESIPT)¹⁹, and optical properties varying in tautomer form. TTz-based fluorophores consisting of two adjacent thiazole rings, have been among the topics of interest in organic electronics due to their planar and rigid structure and superior optical-electronic properties. Interest in TTz compounds has increased dramatically in the last decade, after the reporting of effective studies on their use in optoelectronic devices such as organic light-emitting diodes (OLEDs)²⁰ and organic field effect transistors (OFETs)^{21,22}. After these initial reports, an increasing number of small molecule compounds and polymeric materials containing the thiazolo[5,4-*d*]thiazole unit have been described in the literature. Their applications in various fields, including photovoltaics, have been investigated²³⁻²⁹. Photoluminescent polymeric films with solvatochromic memory³⁰, having phosphorescence at room temperature³¹, radiation-sensitive polymer films as dosimeters³², the use of in-situ SiO₂ synthesized biodegradable films in food packaging³³, fluorescence films for enzyme-free H₂O₂ detection³⁴, temperature sensitive polymer films^{35,36}, polymer films for TNT detection³⁷, erasable fluorescence imaging³⁸ are some intriguing reports showing different applications of such films.

Herein, a new approach is reported to prepare optically anisotropic films having dual color emission in the two sides of the films consisting of nanocrystals and photoluminescent organic dyes. CdSe/CdS NRs were used as orange-red emitter while the 2,5-bis(4-hydroxyphenyl)thiazolo[5,4-*d*]thiazole (HPhTT) molecule was used as blue / green emitter. The synthesized NRs and optically anisotropic films were characterized with TEM imaging, ATR-IR, Raman spectroscopy, spectrophotometric / spectrofluorometric analysis and confocal microscopy. These films are

unique materials for various optical applications such as waveguides or sensors.

2. Materials and Method

2.1. Materials

All chemical solvents and reagents were supplied commercially and used without any further purification. ethanol (96%), 2-(diethylamino)ethyl methacrylate (DEAEMA, 98%), 4-hydroxy benzaldehyde (98%), polyethylene glycol monomethyl ether, glycidyl methacrylate (GMA, 97%), CuCl (99%), and KOH (%85) were purchased from Sigma-Aldrich. CdO (Sigma-Aldrich, 99.9%), trioctyl phosphine (TOP, abcr, 97%), ODPa (abcr, 97%), Se (Sigma-Aldrich, 99.99%), trioctyl phosphine oxide (TOPO, Alfa Aesar, 98%), S (Sigma-Aldrich, 90%), ethanol (Sigma-Aldrich, 99.8%), methanol (Alfa Aesar, 99.9%), THF (Sigma-Aldrich, 99.9%), hexane (Honeywell), toluene (Merck, anhydrous), ethylene glycol (EG, Sigma-Aldrich, 99%) diethylene glycol (DEG, Sigma-Aldrich, 99%) were used. Toluene (99.8%) was from Interlab. Dithiooxamide (98%), α -bromoisobutyryl bromide (BIBB, 98%) were purchased from Acros Organics. Pyridine (99%), triethylamine (99%), tetrahydrofuran (THF, 99%) and hexane (95%) were purchased from Merck. 2,2'-Bipyridine (BPy, 99%) was from Alfa Aesar. Acetic acid (AcOH, 100 %) and KH₂PO₄ (99%) was supplied from Reidel-de Haen. Poly(ethylene glycol) methyl ether (MPEG, 2000 g/mol) was supplied from Fluka.

2.2. Method

2.2.1. Preparation of Se precursor

0.058 g of Se powder and 1.2 g of TOP is put in a 2 ml vial and mixed for 1 hour at 80 °C till all Se powder is dissolved. A colorless homogeneous solution formation indicates the dissolution of Se in TOP.

2.2.2. Synthesis of CdSe seed

Hot injection method was performed by injecting a cold chalcogenide precursor into a high-temperature metal precursor for CdSe quantum dots synthesis. 3.00 g of TOPO, 0.06 g CdO and 0.28 g ODPa are put in a three necked flask inside the glove box for further attachment to the Schenk line in the fumehood. The mixture was melted in N₂(g) atmosphere, then the mixture was stirred for 1 hour under vacuum (4.10⁻² Torr) at 170 °C to remove the oxygene and water in the environment and the chemicals that will inhibit the reaction. Later, the reactants are allowed to interact at 300 °C to form a colorless solution. The temperature is increased to 380 °C for injecting 1.5 g TOP and then Se-TOP precursor. The heating mantle is quickly removed when the color of the solution turns brownish red. The flask is rapidly cooled, and 5 mL of anhydrous toluene is injected. Then, the

quantum dot colloidal solution is precipitated by adding 2 mL of anhydrous methanol twice by centrifugating at 3000 rpm for 10 minutes.

2.2.3. Preparation of S precursor

0.12 g of S powder and 1.5 g of TOP was placed in a 2 ml vial, and stirred at 80 °C for 1 hour to dissolve all S in the TOP. A colorless solution was obtained.

2.2.4. Synthesis of CdSe/CdS NRs

CdSe/CdS NRs were synthesized via seeded growth approach. 0.06 g CdO, 3 g TOPO, 0.34 g OHPA were weighted to put in a three-necked flask. The reactants were kept under vacuum for approximately 1 hour at 170 °C. The mixture was heated to 355 °C. 1.5 g of TOP was injected when it reached the injection temperature, followed by injection of S-TOP and CdSe quantum dot precursors. Crystals were allowed to grow for 6 minutes at this temperature. Rapid cooling of the reaction flask was achieved by water bath. 10 mL of toluene was injected when the temperature dropped to 60 °C. The product was transferred to vials using a syringe. Purification was achieved by centrifugation at 3000 rpm by adding methanol solution³⁹.

2.2.5. Preparation of optically anisotropic films

Optically anisotropic films were prepared at liquid air interface. Ethylene glycol (EG) containing 0.05 g HPhTT dye and 0.005g hexamethylene diamine was used as subphase to form interface. A mixture of NRs and polymer was prepared by dissolving 0.6 g of synthesized MPEG-*b*-PGMA-*b*-DEAEMA block copolymer that is described in our earlier report²⁹ and 200 μ L NRs in 5 mL hydrophobic solvent (i.e. toluene). The mixture was put on top of EG and the solvent was evaporated slowly to form a solid film. The film was removed from the top of the solution and washed with isopropanol to remove unreacted dyes and EG, then they are dried at room temperature.

3. Results and Discussions

Here hot injection method modified by seeded growth approach was used for the synthesis of CdSe/CdS core/shell nanorod by using CdSe QD as seed. Strong and tunable light emission from green to red can be obtained from these CdSe/CdS nanorods having narrow size distributions by this method^{39, 40}. CdSe/CdS NRs with red emission were synthesized by using well-defined CdSe QDs as seed. TEM images of the CdSe QDs and NRs are given in Figure 1-a,b, respectively.

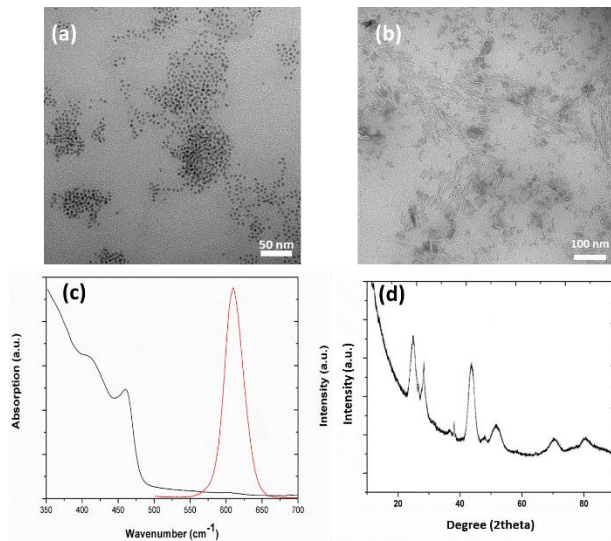


Figure 1. TEM image of CdSe seed (a), CdSe/CdS NRs (b), absorption and PL spectra (c), XRD spectrum (d) of CdSe/CdS NRs (Reference code: 98-065-9045)

The absorption from CdS shell as the high-energy peaks and the lowest energy peak originated from electronic transitions from holes confined in the CdSe seed is given in the absorption spectrum (Figure 2c). Photoluminescence (PL) peak of the NRs is located at 610 nm as shown in Figure 2c [37, 38].

The absorption from CdS shell as the high-energy peaks and the lowest energy peak originated from electronic transitions from holes confined in the CdSe seed is given in the absorption spectrum (Figure 2c). Photoluminescence (PL) peak of the NRs is located at 610 nm as shown in Figure 2c^{39, 41}.

The synthesized NRs were also characterized by X-ray diffraction analysis (Figure 1-d). Cadmium chalcogenide peaks are observed at $2\theta = 24.86^\circ, 26.45^\circ, 28.21^\circ, 36.61^\circ, 43.78^\circ, \text{ and } 51.88^\circ, 71.03^\circ, 83.354^\circ$ which can be assigned to the, (010), (002), (011), (012), (110), (112), (121), (123) reflections, respectively⁴².

The synthesized NRs were used to prepare composite films in the liquid-air interface. In the literature, preparation of colloidal nanocrystal doped polymer films is performed via casting method onto a Petri dish without any phase separation. However, the polymers are consist of commercially available, single chain polymers^{6, 43, 44}. Even there are some reported composite examples of colloidal semiconductor nanocrystals/block copolymers, the films of the composites were prepared via casting method⁴⁵. Here amphiphilic behavior of the block copolymers is used to manage phase separation to get dual-wavelength emission. Dual wavelength emissive materials of colloidal nanocrystals can be prepared by using silica nanoparticles with a sequential deposition method as reported before⁴⁶. Such dual wavelength emissive materials have great attention due to their high

demand in many application fields, such as photonic circuits⁴⁷ biosensors⁴⁸, on-chip optical communication⁴⁹ and bioimaging⁵⁰. In this new method one-step preparation of dual emissive films is achieved by managing solution behavior of block copolymers and nanorods. The nanorods and polymer solution in hydrophobic solvents such as hexane and toluene was used for further slowly evaporation of the solvent to form a solid film on the top of liquid subphase.

HPhTT dye addition to subphase resulted in diffusion of the dye in the polymer films. The diffusion rate is expected to be higher in the contact layer of polymer with the subphase (i.e. liquid interface). The diffusion of the dye decreases at the air interface.

This diffusion gradient results in a phase separated green emission of HPhTT. On the other hand, the highly hydrophobic ligands around the NRs and the amphiphilic behaviour of the polymer limits the interaction of NRs with the subphase.

So, amphiphilic polymer molecules assemble on top of subphase (i.e. liquid interface) similar to surfactant behaviour resulting in the phase separation of NRs from green emission. Digital images of the experimental set up of optically anisotropic film preparation under daylight and UV-light excitation are given in Figure 2 (top) with dual color emission.

The solid films obtained by this method are given in Figure 2 (bottom). The dual color emission from both layers of the films can be seen under UV-light excitation. It is clearly seen that this method results in an anisotropy when the z-axis (i.e. thickness) of the film is observed. HPhTT dye and NRs distribution in the thickness of the film cause an emission or optical anisotropy.

So the films with dual color emission are named as “optically anisotropic films”.

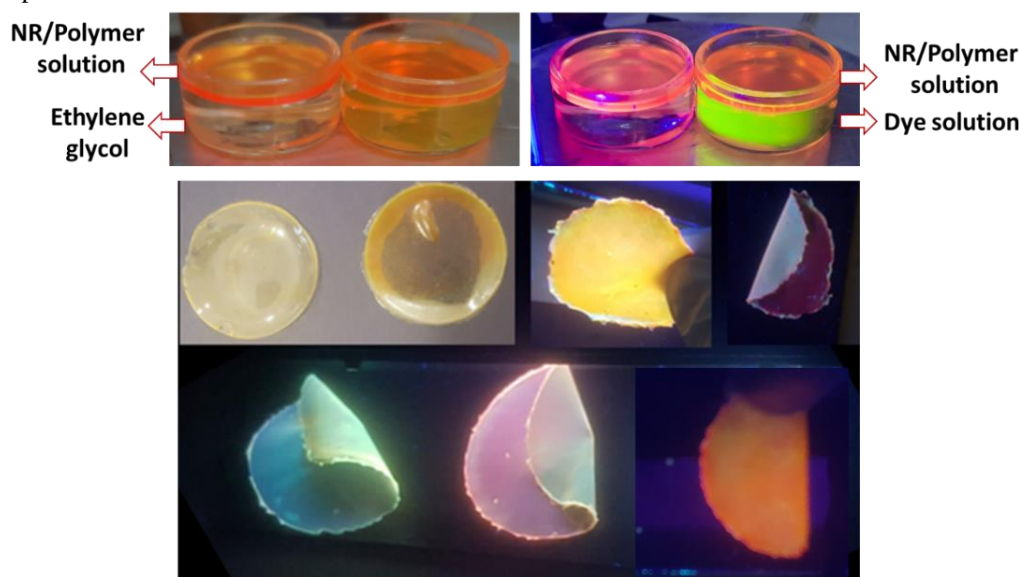


Figure 2. Digital images of optically anisotropic film preparation (top), and the final product films under UV-light excitation (bottom).

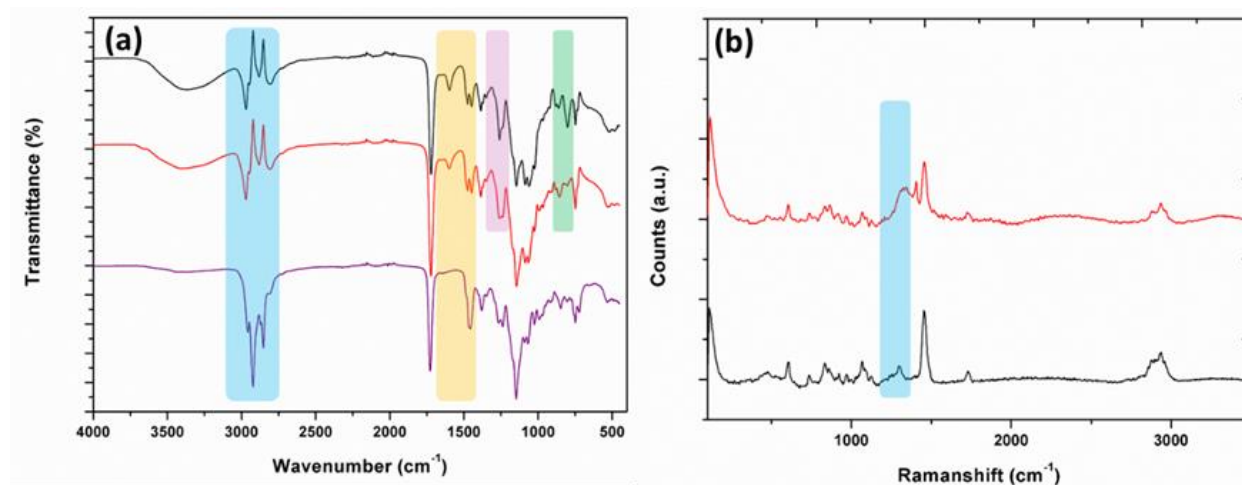


Figure 1. ATR-IR spectra of polymer film (black line), dye loaded film (red line) and dye/NR loaded film (purple line) (a), Raman shift of dye loaded film (black line) and dye/NR loaded film (red line) (b).

The films were investigated by ATR-IR and Raman spectroscopies as given in Figure 3a and b, respectively. Since diffused HPhTT dye amount is too less, the vibrations of the molecule was not observed in ATR-IR spectrum while it is interacted with polymer as observed in the fingerprint region (green and lilac signs). ATR-IR spectrum of the NRs containing optically anisotropic films is given in Figure 3a (purple line). The hydrophobic long chain ligands around the NRs can be observed with the stretching of C-H groups at 2900-3000 cm^{-1} . -C=O stretching is at 1729 cm^{-1} , C-O-C and O-CH₂ stretching is at 1100-1200 cm^{-1} . The two bands at 1387 cm^{-1} and 75 cm^{-1} can be attributed to the α -methyl group vibrations.

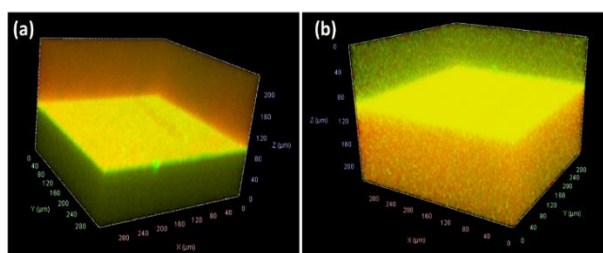


Figure 3. Three dimensional confocal micrographs of optically anisotropic film obtained by z-axis scanning

The confocal micrographs of the dual emissive film obtained by z-scanning of the films from both side (i.e. dye rich or nanorod rich regions) is given in Figure 4a-b. The NR rich region is observed by red area while dye rich region is observed as green region. The yellow color is seen because of overlapping of both colors. It is obviously seen successfully achievement of phase separation of the colors can be obtained by this approach.

4. Conclusion

In conclude, a new method to prepare optically anisotropic films is reported. In this study, it has been shown that new materials can be prepared by subphase modification at the liquid-air interface for various nanostructures. For this purpose, colloidal nanocrystals are synthesized and characterized by spectrophotometric, spectrofluorometric analysis, TEM imaging and X-Ray analysis. The prepared films are also characterized by ATR-IR and Raman spectroscopies.

The bending vibration of the C-H bonds of the -CH_3 group is at 1459 cm^{-1} . Raman shifts of the dye (black line) and dye/NR (red line) loaded films are given in Figure 3b. The peaks between 440 - 465 cm^{-1} are due to the bending vibration of the carbonyl group (-C=O). The epoxide asymmetric ring deformation of PGMA is located at 923 cm^{-1} as a weak band may be attributed to C-H groups of the polymer and ligands around NRs are observed at 2900-3000 cm^{-1} ⁵¹.

The confocal micrographs are given in Figure 4a,b. The two sides of optically anisotropic film is scanned and dye

rich region is shown as green while NR rich region is shown as red.

It is clearly seen that the film is divided to two region because of the forming dye rich and NR rich areas as a result of diffusion rate of dye, hydrophobic nature of NRs and amphiphilic behavior of the polymer. This new method and novel optically anisotropic films pave the way for many optical applications.

Confocal microscopy is also shown to be used effectively for three dimensional imaging of hybrid materials. This method can be adopted for many other materials and such optically anisotropic films are great candidate for optical sensors and waveguides.

The Declaration of Conflict of Interest/ Common Interest

No conflict of interest or common interest has been declared by the author.

Author's Contributions

Zeynep Dikmen: Visualization, Methodology, Conceptualization, Writing – Review & Editing, Validation, Writing – Original Draft, Data Curation Funding Acquisition, Resources.

Ethics

There are no ethical issues after the publication of this manuscript.

Acknowledgement

This study was supported by the Scientific Research Projects Coordination Unit of Eskisehir Osmangazi University (ESOGU BAP) within the scope of the project numbered FCD-2023-2764.

References

- [1]. A. Prudnikau, D. I. Shiman, E. Ksendzov, J. Harwell, E. A. Bolotina, P. A. Nikishau, S. V. Kostjuk, I. D. W. Samuel and V. Lesnyak. 2021. Design of cross-linked polyisobutylene matrix for efficient encapsulation of quantum dots. *Nanoscale Adv*; 3: 1443-1454.
- [2]. B. M. Saidzhonov, V. B. Zaytsev and R. B. Vasiliev. 2021. Effect of PMMA polymer matrix on optical properties of CdSe nanoplatelets. *J Lumin*; 237: 118175.
- [3]. R. Lesyuk, B. Cai, U. Reuter, N. Gaponik, D. Popovych and V. Lesnyak. 2017. Quantum-Dot-in-Polymer Composites via Advanced Surface Engineering. *Small Methods*; 1: 1700189.
- [4]. P. D. Cunningham, J. B. Souza, I. Fedin, C. She, B. Lee and D. V. Talapin. 2016. Assessment of Anisotropic Semiconductor Nanorod and Nanoplatelet Heterostructures with Polarized Emission for Liquid Crystal Display Technology. *Acs Nano*; 10: 5769-5781.
- [5]. İ. Ç. Keskin, M. Türemiş, M. İ. Katı, R. Kibar and A. Çetin. 2019. Effects of CdS quantum dot in polymer nanocomposites: In terms

- of luminescence, optic, and thermal results. *Radiation Physics and Chemistry*; 156: 137-143.
- [6]. S. Cho, J. Kwag, S. Jeong, Y. Baek and S. Kim. 2013. Highly Fluorescent and Stable Quantum Dot-Polymer-Layered Double Hydroxide Composites. *Chem Mater*; 25: 1071-1077.
- [7]. İ. Ç. Keskin, M. Türemiş, M. İ. Katı, R. Kibar, K. Şirin, M. A. Çipiloğlu, M. Kuş, S. Büyükcşelebi and A. Çetin. 2017. The radioluminescence and optical behaviour of nanocomposites with CdSeS quantum dot. *Journal of Luminescence*; 185: 48-54.
- [8]. E. Banks, Y. Okamoto and Y. Ueba. 1980. Synthesis and Characterization of Rare-Earth Metal-Containing Polymers .1. Fluorescent Properties of Ionomers Containing Dy³⁺, Er³⁺, Eu³⁺, and Sm³⁺. *J Appl Polym Sci*; 25: 359-368.
- [9]. H. Lu, G. F. Li, S. B. Fang and Y. Y. Jiang. 1990. Fluorescent Properties of Polymer Rare-Earth Ion Complexes .2. Poly(Acrylic Acid-Co-Acrylamide) Rare-Earth Ion Complexes. *J Appl Polym Sci*; 39: 1389-1398.
- [10]. K. J. Smit and K. P. Ghiggino. 1991. Effect of Polymer Binding on the Spectroscopic Properties of Stilbene-Based Fluorescent Dyes. *J Polym Sci Pol Phys*; 29: 1397-1405.
- [11]. E. Chiellini, R. Solaro, G. Galli and A. Ledwith. 1980. Optically-Active Vinyl-Polymers Containing Fluorescent Groups .8. Synthesis and Properties of Co-Polymers of N-Vinylcarbazole and (-)-Menthyl Acrylate and (-)-Menthyl Methacrylate. *Macromolecules*; 13: 1654-1660.
- [12]. M. Delfini, M. E. Dicocco, M. Paci, R. Solaro and E. Chiellini. 1985. Optically-Active Vinyl-Polymers Containing Fluorescent Groups .9. C-13-Nmr Spectra of Copolymers of (-)-Menthyl Vinyl Ether with N-Vinylcarbazole. *Eur Polym J*; 21: 723-726.
- [13]. R. E. Sah. 1981. Stokes Shift of Fluorescent Dyes in the Doped Polymer Matrix. *J Lumin*; 24-5: 869-872.
- [14]. C. D. Eisenbach. 1983. Characteristic Features of the Matrix Effect on the Stokes Shift of Fluorescent Dye Molecules in Pure and Plasticized Polymers. *J Appl Polym Sci*; 28: 1819-1827.
- [15]. E. T. B. Altakrity, A. D. Jenkins and D. R. M. Walton. 1990. The Synthesis of Polymers Bearing Terminal Fluorescent and Fluorescence-Quenching Groups .2. The Incorporation of Fluorescent and Fluorescence-Quenching Groups by Means of a Direct Termination Process. *Makromol Chem*; 191: 3069-3072.
- [16]. R. P. Quirk, J. G. Kim, K. Rodrigues and W. L. Mattice. 1990. Anionic Synthesis and Characterization of Poly(Styrene-Block-Ethylene Oxide) Polymers with Fluorescent-Probes at the Block Junctions. *Abstr Pap Am Chem S*; 199: 403-Poly.
- [17]. R. P. Quirk, J. Kim, K. Rodrigues and W. L. Mattice. 1991. Anionic Synthesis and Characterization of Poly(Styrene-Block-Ethylene Oxide) Polymers with Fluorescent-Probes at the Block Junctions. *Makromol Chem-M Symp*; 42-3: 463-473.
- [18]. A. Woodward, N. Sayresmith, J. Sailer, K. Sandor and M. Walter. 2019. Fluorescent thiazolothiazole viologen materials for energy storage: Photochemistry, electrochromism, and photoluminescence. *Abstr Pap Am Chem S*; 257.
- [19]. Z. Y. Zhang, Y. A. Chen, W. Y. Hung, W. F. Tang, Y. H. Hsu, C. L. Chen, F. Y. Meng and P. T. Chou. 2016. Control of the Reversibility of Excited-State Intramolecular Proton Transfer (ESIPT) Reaction: Host-Polarity Tuning White Organic Light Emitting Diode on a New Thiazolo[5,4-d]thiazole ESIPT System. *Chem Mater*; 28: 8815-8824.
- [20]. Q. Peng, J. B. Peng, E. T. Kang, K. G. Neoh and Y. Cao. 2005. Synthesis and electroluminescent properties of copolymers based on fluorene and 2,5-di(2-hexyloxyphenyl)thiazolothiazole. *Macromolecules*; 38: 7292-7298.
- [21]. S. Ando, J. Nishida, Y. Inoue, S. Tokito and Y. Yamashita. 2004. Synthesis, physical properties, and field-effect transistors of novel thiophene/thiazolothiazole co-oligomers. *J Mater Chem*; 14: 1787-1790.
- [22]. I. Osaka, G. Sauve, R. Zhang, T. Kowalewski and R. D. McCullough. 2007. Novel thiophene-thiazolothiazole copolymers for organic field-effect transistors. *Adv Mater*; 19: 4160-+.
- [23]. D. Bevk, L. Marin, L. Lutsen, D. Vanderzande and W. Maes. 2013. Thiazolo[5,4-d]thiazoles - promising building blocks in the synthesis of semiconductors for plastic electronics. *Rsc Adv*; 3: 11418-11431.
- [24]. G. Reginato, A. Mordini, L. Zani, M. Calamante and A. Dessi. 2016. Photoactive Compounds Based on the Thiazolo[5,4-d]thiazole Core and Their Application in Organic and Hybrid Photovoltaics. *Eur J Org Chem*; 2016: 233-251.
- [25]. Z. Dikmen and V. Bütün. 2021. Thiazolo thiazole based cross-linker to prepare highly fluorescent smart films with tunable emission wavelength and their multi-responsive usage. *European Polymer Journal*; 159: 110759.
- [26]. Z. Dikmen and V. Bütün. Multi-Analyte Sensitive Fluorophore Cross-Linked Nanofibers Based Antimicrobial Surface Enabling Bacterial Detection and Their Usage as Crystal Growth Template. *Macromolecular Materials and Engineering*; n/a: 2300226.
- [27]. O. Turhan, Z. Dikmen and V. Bütün. 2023. Novel approach to increase chemosensing ability of fluorophore via cross-linked hydrogel film formation. *Journal of Photochemistry and Photobiology A: Chemistry*; 443: 114828.
- [28]. Z. Dikmen, G. Dikmen and V. Bütün. 2023. Fluorophore-assisted green fabrication of flexible and cost-effective Ag nanoparticles decorated PVA nanofibers for SERS based trace detection. *Journal of Photochemistry and Photobiology A: Chemistry*; 445: 115074.
- [29]. Z. Dikmen, O. Turhan, A. Özbal and V. Bütün. 2022. In-situ formation of fluorophore cross-linked micellar thick films and usage as drug delivery material for Propranolol HCl. *Spectrochimica Acta Part A: Molecular and Biomolecular Spectroscopy*; 279: 121452.
- [30]. N. Yamada, H. Noguchi, Y. Orimoto, Y. Kuwahara, M. Takafuji, S. Pathan, R. Oda, A. Mohammadali Rahimli, M. Ahmed Ramazanov and H. Ihara. 2019. Emission-Color Control in Polymer Films by Memorized Fluorescence Solvatochromism in a New Class of Totally Organic Fluorescent Nanogel Particles. *Chemistry – A European Journal*; 25: 10141-10148.
- [31]. Y. Su, S. Z. F. Phua, Y. Li, X. Zhou, D. Jana, G. Liu, W. Q. Lim, W. K. Ong, C. Yang and Y. Zhao. 2018. Ultralong room temperature phosphorescence from amorphous organic materials toward confidential information encryption and decryption. *Sci Adv*; 4: eaas9732.
- [32]. Y. S. Soliman, A. A. Abdel-Fattah, A. A. Hamed and A. M. M. Bayomi. 2018. A radiation-sensitive monomer of 2,4-hexadiyn-1,6-bis(p-toluene sulphonyl urethane) in PVA as a radiochromic film dosimeter. *Radiat Phys Chem*; 144: 56-62.
- [33]. Z. Yu, B. Li, J. Chu and P. Zhang. 2018. Silica in situ enhanced PVA/chitosan biodegradable films for food packages. *Carbohydr Polym*; 184: 214-220.
- [34]. D. Kumar, S. Umrao, H. Mishra, R. R. Srivastava, M. Srivastava, A. Srivastava and S. K. Srivastava. 2017. Eu:Y2O3 highly dispersed fluorescent PVA film as turn off luminescent probe for enzyme free detection of H2O2. *Sensor Actuat B-Chem*; 247: 170-178.



- [35]. H. Kim and J. Y. Chang. 2014. Reversible Thermochromic Polymer Film Embedded with Fluorescent Organogel Nanofibers. *Langmuir*; 30: 13673-13679.
- [36]. G. Kwak, S. Fukao, M. Fujiki, T. Sakaguchi and T. Masuda. 2006. Temperature-Dependent, Static, and Dynamic Fluorescence Properties of Disubstituted Acetylene Polymer Films. *Chem Mater*; 18: 2081-2085.
- [37]. G. He, N. Yan, J. Y. Yang, H. Y. Wang, L. P. Ding, S. W. Yin and Y. Fang. 2011. Pyrene-Containing Conjugated Polymer-Based Fluorescent Films for Highly Sensitive and Selective Sensing of TNT in Aqueous Medium. *Macromolecules*; 44: 4759-4766.
- [38]. S.-J. Lim, B.-K. An and S. Y. Park. 2005. Bistable Photoswitching in the Film of Fluorescent Photochromic Polymer: Enhanced Fluorescence Emission and Its High Contrast Switching. *Macromolecules*; 38: 6236-6239.
- [39]. L. Carbone, C. Nobile, M. De Giorgi, F. D. Sala, G. Morello, P. Pompa, M. Hytch, E. Snoeck, A. Fiore, I. R. Franchini, M. Nadasan, A. F. Silvestre, L. Chiodo, S. Kudera, R. Cingolani, R. Krahne and L. Manna. 2007. Synthesis and Micrometer-Scale Assembly of Colloidal CdSe/CdS Nanorods Prepared by a Seeded Growth Approach. *Nano Letters*; 7: 2942-2950.
- [40]. Z. Dikmen. 2024. Gold-tipped CdSe/CdZnS colloidal quantum wells as non-quenching plasmonic particles for optical applications. *Optical Materials*; 147: 114761.
- [41]. X. Peng, M. C. Schlamp, A. V. Kadavanich and A. P. Alivisatos. 1997. Epitaxial Growth of Highly Luminescent CdSe/CdS Core/Shell Nanocrystals with Photostability and Electronic Accessibility. *Journal of the American Chemical Society*; 119: 7019-7029.
- [42]. T. Duan, J. Ai, X. Cui, X. Feng, Y. Duan, L. Han, J. Jiang and S. Che. 2021. Spontaneous chiral self-assembly of CdSe@CdS nanorods. *Chem*; 7: 2695-2707.
- [43]. W.-C. Wang, H.-Y. Wang, T.-Y. Chen, C.-T. Tsai, C.-H. Cheng, H.-C. Kuo and G.-R. Lin. 2019. CdSe/ZnS core-shell quantum dot assisted color conversion of violet laser diode for white lighting communication. *Nanophotonics*; 8: 2189-2201.
- [44]. N. Yin, S. Zhao, P. Li and L. Liu. 2018. One-pot synthesis of Ag nanoparticle/Ag-doped SiO₂ composite film and their enhancement effect for CdSe QDs. *Functional Materials Letters*; 11: 1950008.
- [45]. J. Wang, C. Guo, Y. Yu, H. Yin, X. Liu and Y. Jiang. 2015. Self-doped 3-hexylthiophene-b-sodium styrene sulfonate block copolymer: synthesis and its organization with CdSe quantum dots. *RSC Advances*; 5: 17905-17914.
- [46]. A. T. Isik, F. Shabani, F. Isik, S. Kumar, S. Delikanli and H. V. Demir. 2023. Simultaneous Dual-Color Amplified Spontaneous Emission and Lasing from Colloidal Quantum Well Gain Media in their Own Layered Waveguide and Cavity. *Laser & Photonics Reviews*; 17: 2300091.
- [47]. M. Athanasiou, R. M. Smith, J. Pugh, Y. Gong, M. J. Cryan and T. Wang. 2017. Monolithically multi-color lasing from an InGaN microdisk on a Si substrate. *Scientific Reports*; 7: 10086.
- [48]. M. Schubert, L. Woolfson, I. R. M. Barnard, A. M. Dorward, B. Casement, A. Morton, G. B. Robertson, P. L. Appleton, G. B. Miles, C. S. Tucker, S. J. Pitt and M. C. Gather. 2020. Monitoring contractility in cardiac tissue with cellular resolution using biointegrated microlasers. *Nature Photonics*; 14: 452-458.
- [49]. S. Han, W. Zhang, B. Qiu, H. Dong, W. Chen, M. Chu, Y. Liu, X. Yang, F. Hu and Y. S. Zhao. 2018. Controlled Assembly of Organic Composite Microdisk/Microwire Heterostructures for Output Coupling of Dual-Color Lasers. *Advanced Optical Materials*; 6: 1701077.
- [50]. T. Pan, D. Lu, H. Xin and B. Li. 2021. Biophotonic probes for bio-detection and imaging. *Light: Science & Applications*; 10: 124.
- [51]. C. Tapeinos, E. K. Efthimiadou, N. Boukos, C. A. Charitidis, M. Koklioti and G. Kordas. 2013. Microspheres as therapeutic delivery agents: synthesis and biological evaluation of pH responsiveness. *Journal of Materials Chemistry B*; 1: 194-203.